Table 4. Stepwise regression analysis

Dependent variable		Independent variable	Intercept	p value
VPS-R	0 POD	EA	1.409	0.0033
	1 POD	EA	1.000	0.0462
	2 POD	–	0.543	–
VPS-M	0 POD	EA, ASA	2.269	<0.0001
	1 POD	EA	1.500	<0.0001
	2 POD	EA, DOS	1.035	0.0017

VPS-R, verbal pain score at rest; VPS-M, verbal pain score on movement; POD, postoperative day; EA, epidural anesthesia; ASA, risk grade according to criteria set down by American Society of Anesthesiology; DOS, duration of surgery.

Table 5. Postoperative complication and side effect of EA

Complication	EA group	NEA group
Nausea/vomiting*	7	1
Pruritus	4	0
Vertigo	1	0
Air leakage (>7 POD)	0	1

POD, postoperative day; EA, epidural anesthesia; NEA, non-EA; *, $p<0.05$.

(NSAIDs), etc. It is important to find the best effect of each analgesic technique. Intravenous injection of narcotics is usually used for perioperative analgesia. However, we did not use intravenous narcotics in this study, because this would have made it difficult to assess the effect of EA due to the strong and long-lasting analgesic effect of narcotics.

Our first hypothesis was that there would be no need to use EA after VATS, because patients who undergo VATS suffer minimal postoperative pain. However, this study showed that patients in the EA group had less postoperative pain and needed less additional analgesics than those of the NEA group in the early postoperative period. While VAS evaluates global pain, VPS-R and VPS-M evaluate pain at rest and on movement, respectively. The incidences of pain between the 2 groups evaluated by VAS, VPS-R and VPS-M were significant at 0 POD, from 0 to 1 POD, and from 0 to 2 POD, respectively. From these results, we believe that EA is effective for control of postoperative pain until 1 POD, although other kinds of analgesics, such as NSAIDs, would be sufficient from 2 POD. It is notable that EA was effective for pain on movement from 0 to 2 POD. Controling pain on movement will improve the ability to deep breathe, cough and walk to prevent atelectasis and pneumonia. Using meta-analysis, Block et al. demonstrated that EA provided better postoperative analgesia than parenteral opioids during the early postoperative period, but not at the 4 POD.[16] Our study obtained similar results in that EA was effective until 1 POD, but that NSAIDs could control postoperaive pain from 2 POD. Nomori et al. stated that prolonged thoracic EA after limited thoracotomy significantly increased the severity of pain after withdrawal.[17] These studies demonstrated that EA should be withdrawn as soon as NSAIDs control postoperative pain.

Several complications of EA have been reported, such as nausea, vomiting, hypotension, pruritus and technical complications.[18] In this study, the patients in the EA group suffered nausea or vomiting more frequently than those in the NEA group. As all patients who complained of nausea or vomiting were over 60 years old, we consider it advisable to discontinue EA from 2 POD, especially in elderly patients.

In conclusion, results suggest that EA is recommended until 1 POD after VATS, and other kinds of analgesics should be employed from 2 POD. However, in patients who complain of side effects due to EA, such as nausea or vomiting, especially in elderly patients, EA should be discontinued within one day after surgery. Although developments have been made recently in VATS, the optimal postoperative analgesic methods have been controversial. We hope this study will help VATS surgeons to decide the optimal postoperative analgesic method.

References

1. Landreneau RJ, Hazelrigg SR, Mack MJ, et al. Postoperative pain-related morbidity: video-assisted thoracic surgery versus thoracotomy. *Ann Thorac Surg* 1993; **56**: 1285–9.

2. Waller DA, Forty J, Morritt GN. Video-assisted thoracoscopic surgery versus thoracotomy for spontaneous pneumothorax. *Ann Thorac Surg* 1994; **58**: 372–7.
3. Stammberger U, Steinacher C, Hillingger S, Schmid RA, Kinsbergen T, Weder W. Early and long-term complaints following video-assisted thoracoscopic surgery: evaluation in 173 patients. *Eur J Cardiothorac Surg* 2000; **18**: 7–11.
4. Nagahiro I, Andou A, Aoe M, Sano Y, Date H, Shimizu N. Pulmonary function, postoperative pain, and serum cytokine level after lobectomy: a comparison of VATS and conventional procedure. *Ann Thorac Surg* 2001; **72**: 362–5.
5. Macrae WA. Chronic pain after surgery. *Br J Anaesth* 2001; **87**: 88–98.
6. Li WW, Lee RL, Lee TW, et al. The impact of thoracic surgical access on early shoulder function: video-assisted thoracic surgery versus posterolateral thoracotomy. *Eur J Cardiothorac Surg* 2003; **23**: 390–6.
7. Benedetti F, Amanzio M, Casadio C, et al. Control of postoperative pain by transcutaneous electrical nerve stimulation after thoracic operations. *Ann Thorac Surg* 1997; **63**: 773–6.
8. Fernandez MI, Martin-Ucar AE, Lee HD, West KJ, Wyatt R, Waller DA. Does a thoracic epidural confer any additional benefit following video-assisted thoracoscopic pleurectomy for primary spontaneous pneumothorax? *Eur J Cardiothorac Surg* 2005; **27**: 671–4.
9. Wu CL, Hurley RW, Anderson GF, Herbert R, Rowlingson AJ, Fleisher LA. Effect of postoperative epidural analgesia on morbidity and mortality following surgery in medicare patients. *Reg Anesth Pain Med* 2004; **29**: 525–33.
10. Hazelrigg SR, Landreneau RJ, Boley TM, et al. The effect of muscle-sparing versus standard posterolateral thoracotomy on pulmonary function, muscle strength, and postoperative pain. *J Thorac Cardiovasc Surg* 1991; **101**: 394–401.
11. Richardson J, Sabanathan S. Pain management in video assisted thoracic surgery: evaluation of localised partial rib resection. A new technique. *J Cardiovasc Surg (Torino)* 1995; **36**: 505–9.
12. Landreneau RJ, Mack MJ, Hazelrigg SR, et al. Prevalence of chronic pain after pulmonary resection by thoracotomy or video-assisted thoracic surgery. *J Thorac Cardiovasc Surg* 1994; **107**: 1079–86.
13. Shuman RL, Peters RM. Epidural anesthesia following thoracotomy in patients with chronic obstructive airway disease. *J Thorac Cardiovasc Surg* 1976; **71**: 82–8.
14. Mulder DS. Pain management principles and anesthesia techniques for thoracoscopy. *Ann Thorac Surg* 1993; **56**: 630–2.
15. Horswell JL. Anesthetic techniques for thoracoscopy. *Ann Thorac Surg* 1993; **56**: 624–9.
16. Block BM, Liu SS, Rowlingson AJ, Cowan AR, Cowan JA Jr, Wu CL. Efficacy of postoperative epidural analgesia: a meta-analysis. *JAMA* 2003; **290**: 2455–63.
17. Nomori H, Horio H, Suemasu K. Comparison of short-term versus long-term epidural analgesia after limited thoracotomy with special reference to pain score, pulmonary function, and respiratory muscle strength. *Surg Today* 2001; **31**: 191–5.
18. Badner NH, Bhandari R, Komar WE. Bupivacaine 0.125% improves continuous postoperative epidural fentanyl analgesia after abdominal or thoracic surgery. *Can J Anaesth* 1994; **41**: 387–92.

Usefulness and complications of computed tomography-guided lipiodol marking for fluoroscopy-assisted thoracoscopic resection of small pulmonary nodules: Experience with 174 nodules

Ken-ichi Watanabe, MD,[a] Hiroaki Nomori, MD, PhD,[b] Takashi Ohtsuka, MD, PhD,[a] Masahiro Kaji, MD, PhD,[a] Tsuguo Naruke, MD, PhD,[a] and Keiichi Suemasu, MD, PhD[a]

Objective: Several techniques have been reported for the localization of small pulmonary nodules in thoracoscopic resection. In the present study we examined the usefulness and complications of computed tomography-guided lipiodol marking for thoracoscopic resection in our experience of 174 nodules.

Methods: Computed tomography-guided lipiodol marking was performed on 174 nodules less than 30 mm in size. Of these nodules, 45 showed ground-glass opacity images and 129 showed solid images on computed tomography. The mean size of the nodules was 10 ± 6 mm (range, 2-30 mm), and their mean depth from the pleural surface was 10 ± 7 mm (range, 0-30 mm). One to 7 days before thoracoscopy, all of the nodules were marked with 0.4 to 0.5 mL of lipiodol by using computed tomography. The marked nodules were grasped with a ring-shaped forceps during fluoroscopy and resected by means of thoracoscopy.

Results: All the nodules could be marked and localized by means of fluoroscopy as a clear spot during thoracoscopic surgery. Complications of the marking were chest pain requiring analgesia in 16 (11%) patients, hemosputum in 11 (6%) patients, pneumothorax in 30 (17%) patients, and hemopneumothorax in 1 (0.6%) patient. Eleven (6%) patients with pneumothorax required drainage, and the patient with hemopneumothorax required an emergency operation. No other complications were observed.

Conclusion: Lipiodol marking is a useful, safe, and inexpensive procedure for localizing ground-glass opacity lesions, small pulmonary nodules, or both for thoracoscopic resection.

From the Department of Thoracic Surgery, Saiseikai Central Hospital Tokyo,[a] Tokyo, Japan, and the Graduate School of Medicine, Kumamoto University,[b] Kumamoto, Japan.

Received for publication Feb 22, 2006; revisions received April 2, 2006; accepted for publication April 20, 2006.

Address for reprints: Hiroaki Nomori, MD, Department of Thoracic Surgery, Graduate School of Medicine, Kumamoto University, 1-1-1 Honjo, Kumamoto 860-8556, Japan (E-mail address: hnomori@qk9.so-net.ne.jp).

J Thorac Cardiovasc Surg 2006;132:320-4

0022-5223/$32.00

doi:10.1016/j.jtcvs.2006.04.012

Recently, small pulmonary nodules have been frequently detected with high-resolution computed tomography (CT).[1,2] Performing a percutaneous or transbronchial biopsy for small pulmonary nodules is often difficult, and hence thoracoscopic surgical techniques have been used in diagnostic excisional biopsies, as well as in therapeutic resection. However, a major factor that limits the success of thoracoscopic resection in the case of small or deeply situated pulmonary nodules is the difficulty in localizing the target nodule because of the lack of digital palpation. Furthermore, a bronchioloalveolar carcinoma with a ground-glass opacity (GGO) finding on CT cannot be palpated or visualized frequently, even in the case of lesions that are located just beneath the visceral pleura. Therefore several techniques have been reported for localization of such small nodules or GGO lesions.[3-18] However, these techniques can result in complications, such as pneumothorax, hemorrhage, and air embolism. Since 1999, we have used CT-guided

Abbreviations and Acronyms
CT = computed tomography
GGO = ground-glass opacity
TTNA = transthoracic needle aspiration

lipiodol marking for the thoracoscopic resection of such lesions. The purpose of our study is to examine the usefulness and safety of this procedure.

Materials and Methods

Eligibility

The CT-guided lipiodol marking was approved by the ethics committee of Saiseikai Central Hospital in January 1999. Written informed consent was obtained from all patients after they discussed the risks and benefits of the procedure with the surgeons. The nodules that were thought to be difficult to localize during thoracoscopy, such as GGO lesions, nodules situated at a considerable depth from the pleural surface, and nodules smaller than 1 cm, were candidates for this procedure. The following nodules were excluded: (1) nodules larger than 30 mm in size; (2) nodules located within the inner two third of the lung; and (3) solid nodules that were larger than 10 mm in size and located within 10 mm from the pleural surface.

Patients

Between January 1999 and June 2005, CT-guided lipiodol marking was performed on 174 pulmonary nodules in 150 patients. The mean age of the patients was 62 ± 11 years (range, 35-84 years). Table 1 shows the characteristics of the nodules. The mean size of the nodules was 10 ± 6 mm (range, 2-30 mm). Their mean distance from the pleural surface was 10 ± 7 mm (range, 0-30 mm). There were 45 GGO lesions and 129 solid lesions. All the nodules were detected with chest CT; however, they could not be detected clearly with chest roentgenograms.

Marking Technique

The procedure used for marking was as follows. After 0.5 mg of atropine and 15 mg of pentazocine was injected, the patients were placed on the CT table in a suitable position (supine or prone). A scaled paper with metal wires was placed firmly on the patient, and the CT scan was performed. The shortest distance from the nodule to the thoracic wall was selected as the injection site (Figure 1, *A*). The site for marker injection was marked on the skin, and the angle and depth of the needle required to reach the nodule were determined. After local anesthesia was administered to the thoracic wall, a 22- or 23-gauge needle was introduced from the point marked on the skin to the nodule, in keeping with the angle and depth measured. The syringe was withdrawn to confirm that no blood had flowed backward, and 0.4 to 0.5 mL of lipiodol (Lipiodol Ultrafluid; Laboratoire Guerbet, Aulnay-Sous-Bois, France), which is generally used as a contrast medium for lymphatic vessels, was then injected in a single shot. The presence of the injected materials was confirmed by means of CT after the marking (Figure 1, *B*). Thoracoscopic surgery was performed 1 to 7 days (mean, 1.7 ± 1.1 days) after marking.

TABLE 1. Characteristics of the nodules

Mean size, mm (range)	10 ± 6 (2-30)
Mean distance from the pleura, mm (range)	10 ± 7 (0-30)
Location	
Right upper lobe	42
Right middle lobe	21
Right lower lobe	37
Left upper lobe	34
Left lower lobe	40
CT findings	
Ground-glass opacity	45
Solid	129

CT, Computed tomography.

Thoracoscopic Resection Technique

Thoracoscopy was performed during one-lung anesthesia by using a double-lumen tube. A C-arm–shaped fluoroscopic unit was used to detect the radiopaque nodules, and the radiopaque nodule was grasped with a ring-shaped forceps during fluoroscopy in multiple projections (Figure 1, *C*). The forceps was then moved in several directions to confirm that the nodule was grasped within a ring of the forceps. The grasped nodule was resected with an endostapler. The resected specimens were removed with a surgical bag. Successive resection of the nodules was confirmed by viewing the radiopaque nodule within the resected specimen during fluoroscopy. The nodules were histologically diagnosed by means of routine intraoperative pathologic examination, with the exception of the GGO lesions that were less than 10 mm in size; these were histologically diagnosed by a permanent section.

Results

All the nodules could be marked with lipiodol on the CT images. Even when the lipiodol could not mark within the nodules, it marked within 10 mm from the nodules, which caused no difficulty in their localization. All the nodules were successfully localized and resected during thoracoscopy without conversion to open thoracotomy. Even a nodule that was marked 7 days before the thoracoscopy could be detected during fluoroscopy as a clear spot. Of the 174 nodules, 107 (61%) were diagnosed as malignant, and 67 (39%) were diagnosed as benign (Table 2). For the 81 patients with primary lung cancers, 48 were followed with thoracoscopic lobectomy, and 10 were followed with thoracoscopic segmentectomy. The other 23 patients did not undergo the additional resection because of bronchioloalveolar cell carcinoma of the intraoperative frozen section, poor risk of the patients, or both. All of the surgical margins in patients treated with thoracoscopic wedge resection showed no malignancy.

Table 3 shows the complications accompanying lipiodol marking. Sixteen (11%) patients had chest pain that required analgesia. Eleven (6%) patients had a little hemosputum. Thirty (17%) patients had pneumothorax, and 11 (6%) of these patients required drainage. One (0.6%) patient had

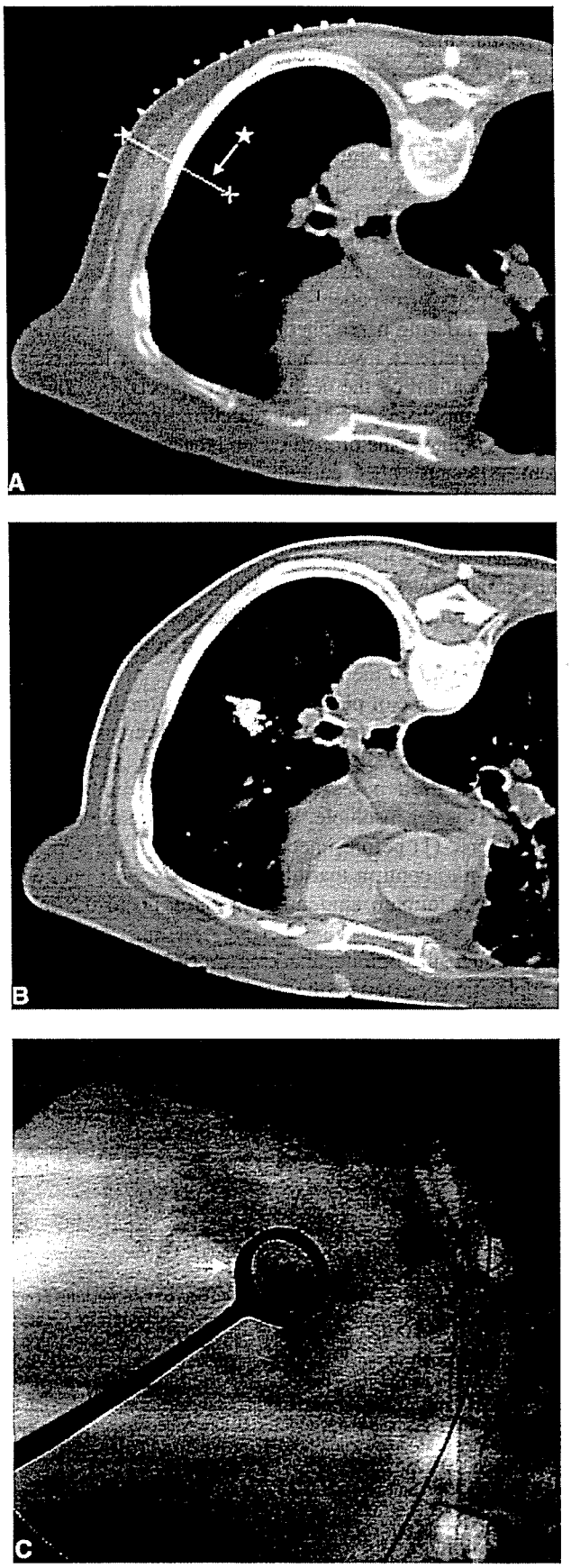

TABLE 2. Pathologic diagnosis of the nodules

Malignant (n = 107)	
Primary lung cancer	81
Metastatic lung cancer	26
Benign (n = 67)	
Tuberculosis	36
Old inflammation	11
Pulmonary lymphoid tissue	9
Atypical adenomatous hyperplasia	8
Hamartoma	3

hemopneumothorax caused by peeling off of the pleural adhesion, including blood vessels.

One patient had bilateral pulmonary nodules, both of which were marked by lipiodol; the patient was given a diagnosis of metastatic colon cancer by means of an ipsilateral thoracoscopy. Therefore the marked contralateral nodule was followed by CT, which had been marked by lipiodol for 3 months.

Discussion

Several methods have been reported for the localization of small pulmonary nodules. These include the hook-wire technique,[3-7] endoscopic ultrasonography,[8,9] barium marking through bronchoscopy,[10,11] and percutaneous injections of dyes,[12,13] colored collagen,[14] lipiodol,[15,16] agar,[17] and barium.[18] The original dye method, because of rapid diffusion around the lung tissue after injection, has the following drawbacks: (1) the marking must be performed within 3 hours before the thoracoscopy to enable dye detection, and therefore both CT and the operating room must be used simultaneously, and (2) the injection site appears blurred because of the diffusion. With the agar marking procedure, it is difficult to localize a deeply situated nodule because the palpation of the marked nodules is requisite. The ultrasound technique requires complete collapse of the lung, which is often impossible in patients with emphysema, resulting in a failure rate of 40% in localizing the nodules.[9] The hook-wire technique has been recently reported to cause massive air embolism,[19-23] which led to its prohibition in Japan. Barium marking with a CT-guided bronchoscopy is complicated because it requires simultaneous use of bronchoscopy and CT, and marking one nodule with this procedure

Figure 1. A, Computed tomographic *(CT)* scan showing a nodule with ground-glass opacity *(GGO)* in the left lower lobe. *The shortest distance from the nodule to the thoracic wall was selected as the injection site. The several lines on the chest wall reveal the metal wires of scaled-paper.* (B) CT showing the tumor marked with lipiodol. C, Intraoperative fluoroscopic imaging showing the radiopaque nodule grasped within a ring-shaped forceps. The nodule is indicated with an *arrow*.

Table 3. Complications of lipiodol marking

	No. of patients (%)
Chest pain requiring analgesia	16 (11)
Hemosputum	11 (6)
Pneumothorax	30 (17)
No treatment	19 (11)
Drainage	11 (6)
Hemopneumothorax	1 (0.6)

requires approximately 30 minutes (range, 15-60 minutes).[11] In addition, barium itself can be seen as a lesion in hematoxylin and eosin–stained sections and also can cause an inflammatory change of the lung tissue, which might make a histologic diagnosis difficult.

We previously marked a nodule with lipiodol and the pleural surface with colored collagen; this enabled a comparatively easier localization of the nodules than when only lipiodol was used.[16] However, 1 mL of collagen costs approximately $80.00. Therefore since March 2002, we started using only lipiodol to mark pulmonary nodules. Thus without using colored collagen, the nodules marked with lipiodol could be localized during fluoroscopy without great difficulty, resulting in a success rate of 100% for thoracoscopic biopsy. The marking procedure with lipiodol has the following advantages: (1) overresection of the normal lung tissue around the nodules was prevented because lipiodol marked the nodules as clear spots that were less than 1 cm in size during fluoroscopy; (2) the lipiodol remained for a long time, up to 3 months after the marking, which solves the problem of requiring both CT and the operating room simultaneously; (3) although the barium marking procedure affects pathologic findings caused by the inflammatory response and barium itself, lipiodol did not affect the pathologic findings; and (4) even in the case of deeply situated nodules (ie, up to 30 mm from the pleural surface in the present study), the lipiodol marking could easily localize the nodules as a clear spot because it diffused only to a small extent.

Transthoracic needle aspiration (TTNA) is also effective in the diagnosis of pulmonary nodules.[24-26] Although TTNA has been reported to have a false-negative rate of 3% to 11%,[24] Layfield and colleagues[25] reported that its diagnostic accuracy decreased to 60% for lesions smaller than 10 mm. Kashiwabara and associates[26] reported that the positive diagnostic rate for nonmalignant lesions by using TTNA was only 56%. All the nodules in the present study were GGO lesions or small nodules deeply situated within the lung, which were not only difficult to diagnose with TTNA but also difficult to locate by means of thoracoscopic inspection without marking. We therefore believe that GGO lesions or small nodules that are deeply situated should be diagnosed by means of thoracoscopic biopsy with preoperative marking.

Although the complications of lipiodol marking included temporary pain, a little hemosputum, pneumothorax, and hemopneumothorax, all of them arose because of the insertion of the needle into the lung and not because of the lipiodol itself. Although we did not encounter air embolism during the lipiodol marking, the frequency of massive air embolism during percutaneous needle insertion into the lung has been reported to be 0.02% to 0.07%.[21] There have been reports of 6 patients who experienced a massive air embolism during percutaneous marking procedures.[19-23] In 5 of the 6 patients, it was caused by the hook-wire technique and in 1 patient by the needle-marker procedure. The massive air embolisms could have occurred because of simultaneous injury of the bronchiole and the adjacent pulmonary vein.[23] Because all 6 patients with massive air embolism had nodules in the lower lobe, we believe that the lung tissue of the lower lobe could be injured more easily by the hook wire or needle marker than that of upper lobe because the former moves more with respiration during insertion of these apparatuses than the latter. Therefore we usually inject lipiodol immediately after needle insertion without confirming the location of the needle tip by means of CT scanning, enabling the time of placing the needle in the lung tissue to be less than 10 seconds, which could decrease the lung damage caused by the needle.

Lipiodol itself poses a potential risk of embolism because it is water insoluble. We therefore take the following precautions: (1) before injection of lipiodol, the syringe is withdrawn to confirm that blood has not flowed backward, and (2) a minimum amount of lipiodol, up to 0.5 mL, is injected.

Although the lipiodol marking procedure showed some complications caused by the needle insertion, they were not of a serious nature. Because it is a simple, safe, and inexpensive method for localizing GGO lesions, small and deeply situated pulmonary nodules, or both, we believe that lipiodol marking is one of the gold standard procedures for localization of these nodules during thoracoscopy.

References

1. Kaneko M, Eguchi K, Ohmatsu H, et al. Peripheral lung cancer: screening and detection with low-dose spiral CT versus radiography. *Radiology.* 1996;201:798-802.
2. Swensen SJ, Jett JR, Hartman TE, et al. CT screening for lung cancer: five-year prospective experience. *Radiology.* 2005;235:259-65.
3. Dendo S, Kanazawa S, Ando A, et al. Preoperative localization of small pulmonary lesions with a short hook wire and suture system: experience with 168 procedures. *Radiology.* 2002;225:511-8.
4. Wicky S, Dusmet M, Doenz F, et al. Computed tomography-guided localization of small lung nodules before video-assisted resection: experience with an efficient hook-wire system. *J Thorac Cardiovasc Surg.* 2002;124:401-3.
5. Mack MJ, Gordon MJ, Postma TW, et al. Percutaneous localization of pulmonary nodules for thoracoscopic lung resection. *Ann Thorac Surg.* 1992;53:1123-4.

6. Plunkett MB, Peterson MS, Landreneau RJ, Ferson PF, Posner MC. Peripheral pulmonary nodules: preoperative percutaneous needle localization with CT guidance. *Radiology.* 1992;185:274-6.
7. Shah RM, Spirn PW, Salazar AM, et al. Localization of peripheral pulmonary nodules for thoracoscopic excision. *Am Roentgenol Surg.* 1992;161:1279-83.
8. Sortini D, Feo CV, Carcoforo P, et al. Thoracoscopic localization techniques for patients with solitary pulmonary nodule and history of malignancy. *Ann Thorac Surg.* 2005;79:258-62.
9. Shennib H, Bret P. Intraoperative transthoracic ultrasonographic localization of occult lung lesions. *Ann Thorac Surg.* 1993;55:67-9.
10. Asano F, Shindoh J, Shigemitsu K, et al. Ultrathin bronchoscopic barium marking with virtual bronchoscopic navigation for fluoroscopy-assisted thoracoscopic surgery. *Chest.* 2004;126:1687-93.
11. Okamura T, Kondo H, Suzuki K, et al. Fluoroscopy-assisted thoracoscopic surgery after computed tomography-guided bronchoscopic barium marking. *Ann Thorac Surg.* 2001;71:439-42.
12. Endo M, Kotani Y, Satouchi M, et al. CT fluoroscopy-guided bronchoscopic dye marking for resection of small peripheral pulmonary nodules. *Chest.* 2004;125:1747-52.
13. Kerrigan DC, Spence PA, Crittenden MD, Tripp MD. Methylene blue guidance for simplified resection of a lung lesion. *Ann Thorac Surg.* 1992;53:163-4.
14. Nomori H, Horio H. Colored collagen is a long-lasting point marker for small pulmonary nodules in thoracoscopic operations. *Ann Thorac Surg.* 1996;61:1070-3.
15. Moon SW, Wang YP, Jo KH, et al. Fluoroscopy-aided thoracoscopic resection of pulmonary nodule localized with contrast media. *Ann Thorac Surg.* 1999;68:1815-20.
16. Nomori H, Horio H, Naruke T, et al. Fluoroscopy-assisted thoracoscopic resection of lung nodules marked with lipiodol. *Ann Thorac Surg.* 2002;74:170-3.
17. Tsuchida M, Yamato Y, Aoki T, et al. CT-guided agar marking for localization of nonpalpable peripheral pulmonary lesions. *Chest.* 1999; 116:139-43.
18. Iwasaki Y, Nagata K, Yuba T, et al. Fluoroscopy-guided barium marking for localizing small pulmonary lesions before video-assisted thoracic surgery. *Respir Med.* 2005;99:285-9.
19. Kamiyoshihara M, Sakata K, Ishikawa S, et al. Cerebral arterial air embolism following CT-guided lung needle marking. Report of a case. *J Cardiovasc Surg (Torino).* 2001;42:699-700.
20. Horan TA, Pinheiro PM, Araujo LM, et al. Massive gas embolism during pulmonary nodule hook wire localization. *Ann Thorac Surg.* 2002;73:1647-9.
21. Sakiyama S, Kondo K, Matsuoka H, et al. Fatal air embolism during computed tomography-guided pulmonary marking with a hook-type marker. *J Thorac Cardiovasc Surg.* 2003;126:1207-9.
22. Sato K, Miyauchi K, Shikata F, et al. Arterial air embolism during percutaneous pulmonary marking under computed tomography guidance. *Jpn J Thorac Cardiovasc Surg.* 2005;53:404-6.
23. Ohi S, Itoh Y, Neyatani H, et al. [Air embolism following computed tomography-guided lung needle marking; report of a case]. *Kyobu Geka.* 2004;57:421-3.
24. Sisler GE. Malignant tumors of the lung: role of video-assisted thoracic surgery. *Chest Surg Clin North Am.* 1993;3:307-17.
25. Layfield LJ, Coogan A, Johnston WW, et al. Transthoracic fine needle aspiration biopsy: sensitivity in relation to guidance technique and lesion size and location. *Acta Cytol.* 1996;40:687-90.
26. Kashiwabara K, Nakamura H, Fukai Y, et al. Availability of diagnosis by percutaneous needle aspiration cytology of the lung in cases who showed a peripheral solitary tumorous shadow on chest Xp and diagnostic rate of transbroncial approach. *Jpn J Thorac Dis.* 1993;31: 1426-31.

GTS

Case Report

Kissing Pleural Metastases from Metastatic Osteosarcoma of the Lung

Takeshi Mori, MD, Masakazu Yoshioka, MD, Kazunori Iwatani, MD, Hironori Kobayashi, MD, Kentaro Yoshimoto, MD, and Hiroaki Nomori, MD, PhD

Two patients with osteosarcoma lung metastases of which migrated to the parietal pleura due to contact are reported. The first patient was a 16-year-old male who had a pleural metastasis in the diaphragm within an area in contact with a single lung metastasis. Both of the tumors were resected, followed by systemic chemotherapy. Nine months after the resection of the first metastases, two other lung metastases were found which were resected after chemotherapy. The patient is alive without recurrence 84 months after the first resection of the metastases. The second patient was an 11-year-old female with a pleural metastasis of osteosarcoma which was within an area in contact with a single lung metastasis, which had been resected 4 months before. We concluded (1) that a lung metastasis of osteosarcoma occasionally metastasizes to the pleura due to contact; and (2) that because this kissing metastases of osteosarcoma could be cured by a complete resection, the intrathoracic cavity should be thoroughly observed. (Ann Thorac Cardiovasc Surg 2006; 12: 129–32)

Key words: metastasectomy, lung, pleura

Introduction

The lung is the most popular metastatic site of osteosarcoma. Jeffree et al. reported that osteosarcoma metastasized to the lung in over 90% of patients who died of osteosarcoma.[1] According to the Japan Autopsy Annual Database, 643 patients died of osteosarcoma between 1981 and 2002 in Japan.[2] Of the 643 patients, 78 (12.1%) had pleural metastases. We present two patients with metastases of parietal pleura which probably originated from a lung metastasis contacting the pleura, namely 'kissing metastases'.

Case Report

Case 1

A 16-year-old male with femoral osteosarcoma received preoperative chemotherapy with cisplatin (CDDP) and doxorubicin (DXR), followed by an extended resection of the right femur and reconstruction in July 1997. Adjuvant chemotherapy with CDDP and cyclophosphamide (CPA) was continued for a total of 10 courses until June 1998. In September 1998, a single lung metastasis in the right lower lobe was found with computed tomography (CT) (Fig. 1). A needle biopsy was not performed. Thoracoscopy showed that a lung metastasis was located in the right lower lobe, and that it was exposed on the surface of the visceral pleura. Additionally, a solitary pleural tumor, 3 mm in size, was found on the diaphragm (Fig. 2). Although these two tumors were separated from each other, the pleural tumor was in an area that was in contact with the pulmonary tumor during ordinary lung expansion in ventilation. Both the lung and pleural tumors were resected. Pathological examination showed that both of the tumors were metastatic osteosarcoma, and that they were covered with a fibrous capsule but not with mesothelial epithelium. Adjuvant chemotherapy with ifosfamide (IFO) and DXR was administered after the first metastasectomy. In July of 1999, two additional lung metastases were detected by CT in the right upper and middle lobes. After chemotherapy with CPA, both me-

From Department of Thoracic Surgery, Kumamoto University Graduate School of Medical Sciences, Kumamoto, Japan

Received September 5, 2005; accepted for publication October 21, 2005.

Address reprint requests to Takeshi Mori, MD: Department of Thoracic Surgery, Kumamoto University Graduate School of Medical Sciences, 1-1-1 Honjo, Kumamoto 860-8556, Japan.

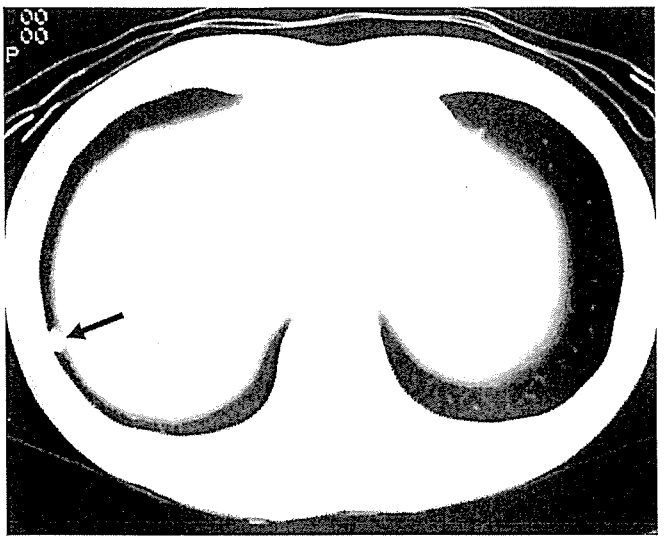

Fig. 1. Case 1.
Computed tomography showing a single lung metastasis (arrow) in the right lower lobe near the pleura.

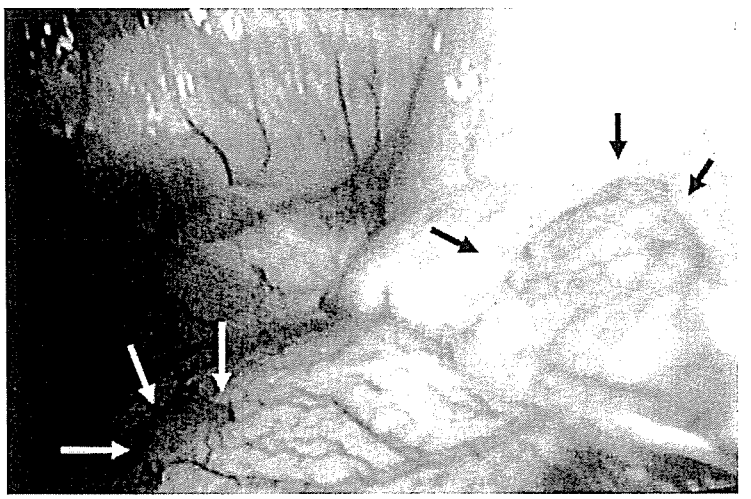

Fig. 2. Case 1.
The lung metastasis was located in the right lower lobe and was exposed on the visceral pleura (black arrows). The pleural metastasis was noted on the diaphragm which was in the area in contact with the lung metastasis (white arrows).

tastases were resected via thoracoscopy, but there were no pleural tumors at that time. Eighty one months after the first resection of metastases, the patient is alive and has not had a recurrence.

Case 2

An 11-year-old female with femoral osteosarcoma underwent preoperative chemotherapy with CDDP and DXR, followed by an extended resection of the left femur and reconstruction in February 2003. Adjuvant chemotherapy with CDDP and CPA was administered for a total of 10 courses until January 2004. In October 2004, a single lung metastasis was found in the right lower lobe by CT. A needle biopsy was not performed. The thoracoscopy showed a lung metastasis which was located in the right lower lobe which was exposed on the visceral pleura. Precise observation of the intrathoracic wall showed no other tumor on either the parietal or visceral pleura. The tumor was resected, followed by chemotherapy with IFO. The pathological diagnosis of the tumor was metastatic osteosarcoma. In March 2005, a pleural metastasis was found by CT (Fig. 3). The thoracoscopy showed a metastasis, 5.3 cm in size, located at the parietal pleura, within the area which was in contact with the scar of the first metastasectomy (Fig. 4). The pleural metastasis was completely resected with intercostals muscle. The pathological examination showed that the tumor was metastatic osteosarcoma and that it was covered with a fibrous capsule but not by mesothelial epithelium. The patient is now alive without recurrence 3 months after the last surgery.

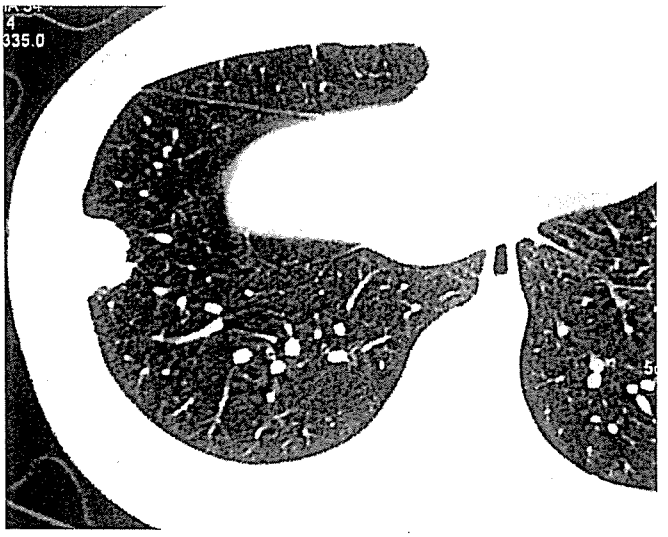

Fig. 3. Case 2.
Computed tomography of the pleural tumor showing extrapleural signs.

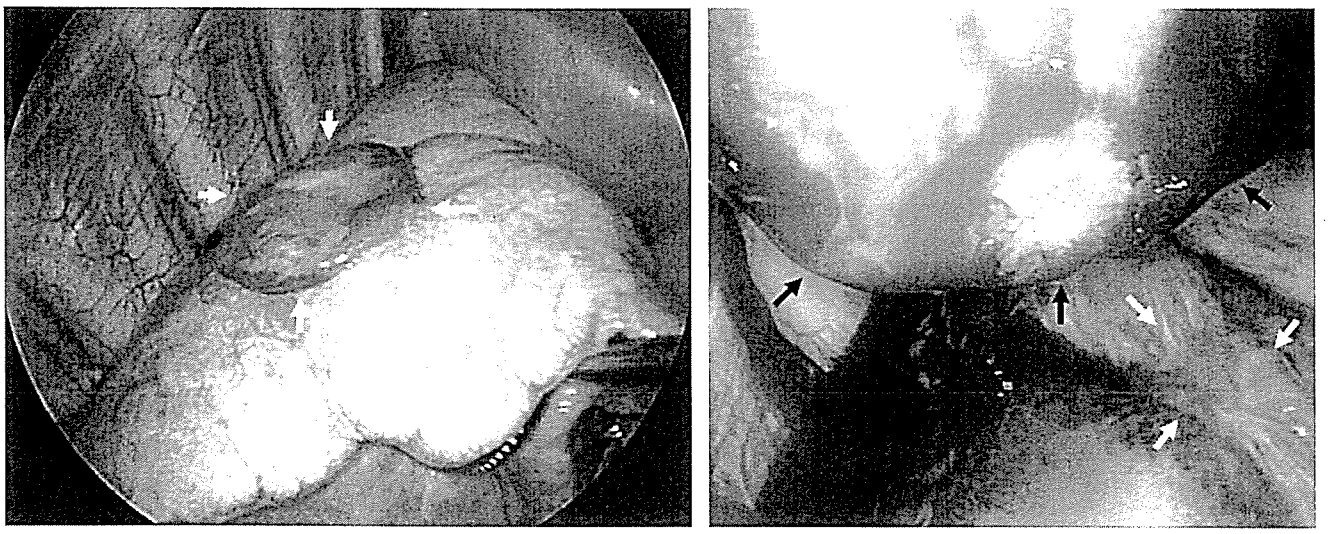

A B

Fig. 4. Case 2.
A: The metastatic pleural tumor which was exposed on the surface of the lung at first metastasectomy (arrows).
B: The metastatic pleural tumor (black arrows) was located on the parietal pleura in front of the scar (white arrows) of the first metastasectomy.

Discussion

As far as we have reviewed, pleural metastasis due to contact with a lung metastasis of osteosarcoma has not yet been reported. Although the pleural metastases in these two patients may have been hematogenous, we believe that both pleural metastases occurred as a result of contact with the previous lung metastases for the following reasons: (1) Although the lung metastasis and pleural metastasis were completely separated from each other in both of the two patients, the pleural metastases were within an area in contact with the lung metastasis during ordinary lung expansion in ventilation; and (2) Both the lung and pleural metastases in the two patients were covered with a fibrous capsule but not by mesothelial epithelium; and (3) After resection of the pleural metastasis, the first patient has not suffered another pleural metastasis or dissemination for over 6 years, which could be explained by the pleural metastasis originating from contact with the lung tumor rather than a hematogenous metastasis or a

dissemination. Although we do not entirely deny the possibility of a hematogenous metastasis or dissemination, it can be surmised that the pleural metastasis of osteosarcoma could occasionally originate from a 'kissing metastases' to the pleura near the site of the lung metastasis, as in the present two cases. While patients with lung metastasis from osteosarcoma usually had bloody pleural effusion, pleural metastasis was rarely found with lung metastasis of osteosarcoma, which was contrary to lung metastasis from carcinoma. Although kissing pleural metastases of osteosarcoma have not been reported before, Nomori et al. reported a patient with a kissing metastases of a fibrous tumor of the pleura.[3] We believe that the kissing metastases could also occur in other kinds of intrathoracic neoplasms, especially in sarcoma rather than carcinoma.

Skinner et al. reported that a 5-year survival rate in the patients with pulmonary metastases of osteosarcoma was 41% after metastasectomy and systemic chemotherapy.[4] Because a kissing pleural metastases of osteosarcoma can be cured after complete resection, we conclude that the pleural cavity in contact with the lung metastasis should be thoroughly observed under a thoracoscopy. Whenever a metastasizing pleural tumor is found within the area in contact with the lung metastasis, the lesions and the surrounding pleura should be resected completely, which could improve the prognosis of patients.

References

1. Jeffree GM, Price CH, Sissons HA. The metastatic patterns of osteosarcoma. *Br J Cancer* 1975; **32**: 87–107.
2. Japanese Society of Pathology. Japan Autopsy Annual Database. Tokyo: Japanese Society of Pathology. (in Jpse.)
3. Nomori H, Horio H, Fuyuno G, Morinaga S. Contacting metastasis of a fibrous tumor of the pleura. *Eur J Cardiothorac Surg* 1997; **12**: 928–30.
4. Skinner KA, Eilber FR, Holmes EC, Eckardt J, Rosen G. Surgical treatment and chemotherapy for pulmonary metastases from osteosarcoma. *Arch Surg* 1992; **127**: 1065–71.

Ann Thorac Surg
2006;81:1132–4

Positive Imaging of Thymoma by 11C-Acetate Positron Emission Tomography

Takashi Ohtsuka, MD, Hiroaki Nomori, MD, PhD, Kenichi Watanabe, MD, Tsuguo Naruke, MD, PhD, Keiichi Suemasu, MD, PhD, Noboru Kosaka, MD, PhD, and Kimiichi Uno, MD, PhD

Department of Thoracic Surgery and Saiseikai Central Hospital, and Nishidai Clinic, Tokyo, Japan

Several studies have shown that fluorine-18 fluorodeoxyglucose (FDG) positron emission tomography (PET) is not useful for the diagnosis of thymoma. We describe 3 patients with thymoma who underwent both FDG-PET

Accepted for publication Jan 5, 2005.

Address correspondence to Dr Ohtsuka, Department of Thoracic Surgery, Saiseikai Central Hospital, 1-4-17 Mita, Minato-ku, Tokyo, 108-0073 Japan; e-mail: t-oh@remus.dti.ne.jp.

0003-4975/06/$32.00
doi:10.1016/j.athoracsur.2005.01.024

and carbon-11 (11C) acetate (AC)-PET. Although all three thymomas were successfully imaged by AC-PET, one of the thymomas was not imaged by FDG-PET. These results suggest that AC-PET may have a potentially important role in the diagnosis of thymoma. This is the first report of the use of AC-PET for diagnostic imaging of thymoma.

(Ann Thorac Surg 2006;81:1132–4)

Recently, carbon-11 (11C) acetate (AC)-PET has been reported to be of clinical value for the diagnosis of cancers that are not imaged by fluorine-18 fluorodeoxyglucose (FDG)-PET, such as prostate cancer and hepatocellular carcinoma [1, 2]. Here we describe three cases of thymoma that were imaged by AC-PET.

Case Reports

Between June and September 2004, 3 patients with thymomas underwent whole-body FDG-PET and AC-PET. The characteristics of the 3 patients are summarized in Table 1. After obtaining the patients' informed consent, AC-PET was performed before FDG-PET on the same day. The dosage of 11C acetate administered was 125 μCi/kg (4.6 MBq/kg). Positron emission tomographic imaging was performed approximately 10 minutes after administration of AC using a POSICAM.HZL mPOWER (Positron Co, Houston, Texas). The emission scans were initially obtained in two-dimensional mode for 4 minutes per bed position and taken from the top of the skull to the thighs. Approximately 30 minutes after AC-positron emission tomographic imaging, fluorine-18 FDG was administered (ie, more than 120 minutes after administration of the acetate). The dosage of FDG was 125 μCi/kg (4.6 MBq/kg) for nondiabetic patients and 150 μCi/kg (5.6 MBq/kg) for diabetic patients, as we reported previously [3]. The FDG-PET scans were performed approximately 45 minutes after administration of FDG. The images were reconstructed using the emission scans and the preinjection transmission scans in a 128 × 128 matrix by ordered subset expectation maximization corresponding to a pixel size of 4 × 4 mm, with a section spacing of 2.56 mm.

Patient 1

Chest computed tomography (CT) showed a tumor located in the anterior mediastinum, measured 3 × 3 cm (Fig 1A). An AC-positron emission tomographic scan showed accumulation at the tumor site with a standardized uptake value (SUV) of 3.5 (Fig 1B), although FDG-PET showed no accumulation with an SUV of 1.0 (Fig 1C). Thymothymectomy was performed, and histopathologic examination showed a thymoma (World Health Organization [WHO] type AB), which had invaded the capsule.

Patient 2

Chest CT showed a tumor measuring 4 × 4 cm located in the anterior mediastinum (Fig 1D). An 11C-acetate PET showed accumulation at the tumor site with an SUV of 2.7. (Fig 1E), and FDG-PET also showed accumulation at the tumor site with an SUV of 5.9 (Fig 1F). Thymothymectomy was performed and histopathologic examination showed a thymoma (WHO type B1) that had invaded the capsule.

Patient 3

Chest CT showed a tumor located in the anterior mediastinum, measuring 7 × 7 cm (Fig 1G). An AC-PET showed strong accumulation at the tumor site with an SUV of 5.9 (Fig 1H), although FDG-PET showed accumulation with an SUV of 3.1 (Fig 1I). Thymothymectomy was performed, and histopathologic examination showed a thymoma (WHO type AB) that had invaded the capsule.

Comment

Thymic tumors are the most common tumors arising in the anterior mediastinum. Clinically the diagnosis of thymic tumors is performed mainly by morphologic examinations, such as CT and magnetic resonance imaging (MRI). Although both CT and MRI have also been reported to be useful for the differential diagnosis of thymic tumors [4], such diagnosis still remains difficult in some cases. FDG-PET has been reported to show high uptake of FDG in thymic cancer, but not in thymoma [5], probably due to its slow growth [6], and low glucose uptake. In the present report we have described three patients of thymomas that were positively imaged by AC-PET. Acetate has been used as a positron-emitting tracer for measurement of oxidative metabolism in the myocardium. The mechanism by which acetate shows high accumulation in tumor cells is still unknown, although it is considered to differ from that of myocardial uptake [7, 8]. Several studies have shown that 11C acetate has higher sensitivity for the detection of prostate cancer [2] and higher sensitivity and specificity for the diagnosis

Table 1. Characteristics of 3 Thymoma Patients

			Standardized Uptake Value				
	Sex	Age	Acetate Positron Emission Tomography	Fluorodeoxyglucose Positron Emission Tomography	Tumor size (cm)	TNM	Histologic Subtype (World Health Organization)
Patient 1	Male	56	3.5	1.0	3 × 3	T2N0M0	AB
Patient 2	Male	35	2.7	5.9	4 × 4	T2N0M0	B1
Patient 3	Female	65	5.9	3.1	7 × 7	T2N0M0	AB

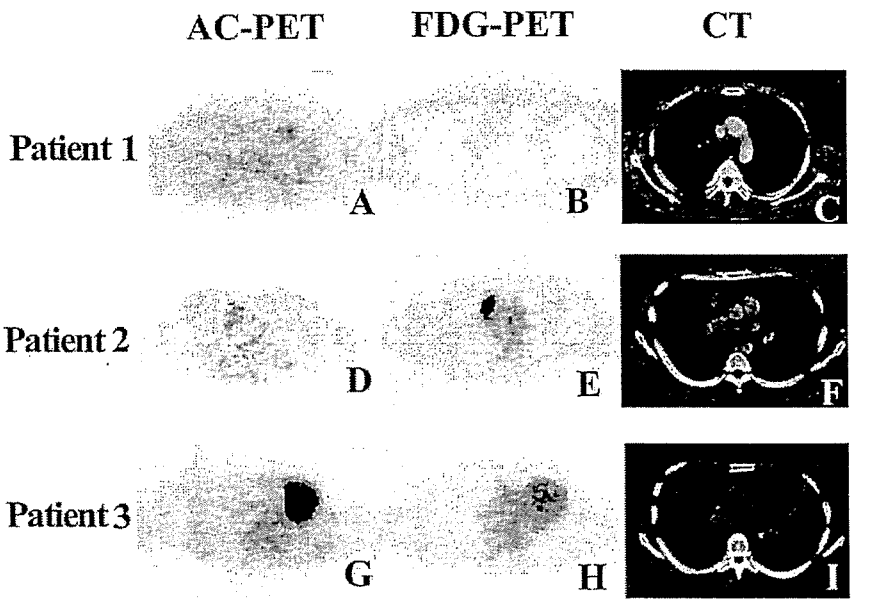

Fig 1. Acetate-positron emission tomography (AC-PET), fluorodeoxyglucose-positron emission tomography (FDG-PET), and computed tomography (CT) in 3 thymoma patients. All 3 thymomas were successfully imaged by AC-PET (A, D, G). By FDG-PET, 2 patients were imaged (E, H), but one was not imaged (B). Chest CT showed anterior mediastinal tumors (C, F, I).

of well-differentiated hepatocellular carcinoma than FDG-PET [1]. Higashi and colleagues [8] described a case of bronchioloalveolar carcinoma in which FDG-PET showed lower uptake than the AC-PET did, suggesting that acetate might accumulate in slow-growing tumors.

We have demonstrated that three patients of thymoma were positively imaged by AC-PET despite showing different results with FDG-PET. Our findings suggest that AC-PET may have a potentially important role in the diagnosis of thymoma, as is the case for other slow-growing tumors such as prostate cancer and bronchioloalveolar carcinoma.

References

1. Ho CL, Yu SC, Yeung DW. 11C-acetate PET imaging in hepatocellular carcinoma and other liver masses. J Nucl Med 2003;44:213–21.
2. Oyama N, Akino H, Kanamaru H, et al. 11C-acetate PET imaging of prostate cancer. J Nucl Med 2002;43:181–6.
3. Nomori H, Watanabe K, Ohtsuka T, Naruke T, Suemasu K, Uno K. Evaluation of F-18 fluorodeoxyglucose (FDG) PET scanning for pulmonary nodules less than 3 cm in diameter, with special reference to the CT images. Lung Cancer 2004; 45:19–27.
4. Molina PL, Siegel MJ, Glazer HS. Thymic masses on MR imaging. AJR Am J Roentgenol 1990;155:495–500.
5. Sasaki M, Kuwabara Y, Ichiya Y, et al. Differential diagnosis of thymic tumors using a combination of 11C-methionine PET and FDG PET. J Nucl Med 1999;40:1595–601.
6. Lewis JE, Wick MR, Scheithauer BW, Bernatz PE, Taylor WF. Thymoma: a clinicopathologic review. Cancer 1987;60:2727–43.
7. Yoshimoto M, Waki A, Yonekura Y, et al. Characterization of acetate metabolism in tumor cells in relation to cell proliferation: acetate metabolism in tumor cells. Nucl Med Biol 2001;28:117–22.
8. Higashi K, Ueda Y, Matsunari I, et al. 11C-acetate PET imaging of lung cancer: comparison with 18F-FDG PET and 99mTc-MIBI SPET. Eur J Nucl Med Mol Imaging 2004;31:13–21.

0003-4975/06/$32.00
doi:10.1016/j.athoracsur.2005.02.093

Sentinel node identification in clinical stage Ia non–small cell lung cancer by a combined single photon emission computed tomography/computed tomography system

Hiroaki Nomori, MD, PhD,[a] Koei Ikeda, MD, PhD,[a] Takeshi Mori, MD, PhD,[a] Shinya Shiraishi, MD, PhD,[b] Hironori Kobayashi, MD,[a] Kazunori Iwatani, MD,[a] Koichi Kawanaka, MD, PhD,[b] and Toshiaki Kobayashi, MD, PhD[c]

From the right to the left: Dr. Ikeda, Dr. Mori, and Dr. Nomori. The bronze statue is Dr. Shibasaburo Kitasato

Objective: A gamma probe can identify sentinel nodes before nodal dissection in the mediastinum but not in the hilum owing to high radioactivity from primary tumors. We evaluated the utility of fused single photon emission computed tomography/computed tomography (SPECT/CT) images for the identification of sentinel nodes in the hilum for patients with clinical stage Ia non–small cell lung cancer.

Methods: Technetium-99m tin colloid was injected into the peritumoral region approximately 18 hours before surgery in 63 patients with clinical stage Ia non–small cell lung cancer. On the morning of the operation, approximately 16 hours after administration of tin colloid, sentinel nodes were identified by fused SPECT/CT; this was followed by intraoperative sentinel node identification in the dissected lymph nodes by gamma probe. Because the gamma probe is a standard method for sentinel node identification, the sensitivity of fused SPECT/CT images was examined on the basis of the data of the gamma probe.

Results: Fused SPECT/CT images could identify sentinel nodes at segmental and lobar lymph nodes with a sensitivity of 0.87 and 0.74, both of which were significantly higher than 0.40 in the mediastinum ($P < .001$ and $P = .012$, respectively). In 5 patients with pathologic N1 or N2 disease, both SPECT/CT and the gamma probe could identify sentinel nodes with metastases.

Conclusions: SPECT/CT could identify sentinel nodes of the hilum especially in segmental and lobar lymph nodes but not in the mediastinum. Because the gamma probe can identify sentinel nodes before nodal dissection in the mediastinum but not in the hilum, a combination of SPECT/CT and the gamma probe can be used to identify sentinel nodes before nodal dissection in both the hilum and the mediastinum, which will enable sentinel node navigation surgery in non–small cell lung cancer.

From the Departments of Thoracic Surgery[a] and Radiology,[b] Graduate School of Medical Sciences, Kumamoto University, Honjo, Kumamoto, and the [c]Department of Assistive Diagnostic Technology, National Cancer Center Hospital, Tsukiji, Chuo-ku, Tokyo, Japan.

Received for publication Dec 3, 2006; revisions received Jan 21, 2007; accepted for publication Feb 7, 2007.

Address for reprints: Hiroaki Nomori, MD, PhD, Department of Thoracic Surgery, Graduate School of Medical Sciences, Kumamoto University, 1-1-1 Honjo, Kumamoto 860-8556, Japan (E-mail: hnomori@qk9.so-net.ne.jp).

J Thorac Cardiovasc Surg ■■■■;■■:■■■

0022-5223/$32.00

doi:10.1016/j.jtcvs.2007.02.013

Sentinel lymph node (SN) sampling with a gamma probe has allowed surgeons to be more selective in performing a formal lymph node dissection in melanoma, breast cancer, and gastrointestinal cancers.[1-3] However, the gamma probe method in lung cancer surgery cannot identify SNs before lymph node dissection in the hilum owing to high radioactivity from primary tumors.[4,5] Therefore, previously reported SN identifications with the gamma probe method in lung cancer surgery have been based on radioactivity measured in the dissected lymph nodes,[5-10] which cannot be used to guide lymph node dissection or sampling. This difficulty with the gamma probe method makes it difficult for SN navigation surgery to be of practical use in non–small cell lung cancer (NSCLC).

Planar scintigram with a radioactive colloid has also been used to identify SNs, especially in melanoma of the head and neck.[11-13] However, in lung cancer surgery, localization of nodal stations by planar scintigram is difficult because SNs cannot

Subject Codes = 10;13

GTS

Abbreviations and Acronyms
CT = computed tomography
NSCLC = non–small cell lung cancer
SN = sentinel lymph node
SPECT = single photon emission computed tomography
^{99m}Tc = technetium-99m

readily be discriminated owing to the lack of tomography images. In 2002, we installed a combined single photon emission computed tomography/computed tomography (SPECT/CT) system that is composed of a gantry-free gamma camera and an 8-row multidetector CT. So that we can avoid positional differences between the SPECT and CT studies, imaging is performed on the same platform, which makes fusion of SPECT and high-performance CT images possible. Because the SPECT/CT system has enabled us to identify SNs on the basis of the fusion images, without the adverse effect of overlapping radioactivity from the primary site, it allows preoperative SN localization in relation to nearby anatomic structures, which enables an intraoperative SN biopsy to be easy and accurate. We[14] previously identified SNs in 35 patients with melanoma by the SPECT/CT system; the identification rate was 100%.[14] The present study evaluated the usefulness of fused SPECT/CT images, compared with the gamma probe, for SN identification in lung cancer surgery.

Patients and Methods

Patient Eligibility

This study of SN identification in patients with clinical stage Ia NSCLC was approved by the ethical committee of the Graduate School of Medical Sciences, Kumamoto University, in March 2005. Clinical staging was performed by body CT, brain magnetic resonance imaging, and positron emission tomography. Informed consent was obtained from all patients after a discussion with the surgeons regarding the risks and benefits. Eligible patients had clinical stage Ia peripheral type NSCLC and were candidates for lobectomy or segmentectomy with mediastinal lymph node dissection. The patients without preoperative histologic diagnosis of tumors were excluded. The lobectomy with mediastinal lymph node dissection was performed via thoracoscopy, as described before.[15] Segmentectomy with hilar and mediastinal lymph node dissection was performed via open thoracotomy, as described before.[16] All of the lymph nodes at the hilum were dissected during segmentectomy with taping of the vessels and bronchus.

Lymph Node Nomenclature

The lymph node nomenclature used was based on the original lymph node map for lung cancer.[17]

Administration of Radioactive Colloid

Administration of the radioactive colloid was based on the method reported previously.[4,5] In the SPECT/CT room, approximately 18 hours before the operation, 6 to 8 mCi of technetium-99m (^{99m}Tc) tin colloid suspended in a volume of 1 to 1.5 mL was injected into the peritumoral region.

SPECT/CT System

On the morning of the operation, approximately 16 hours after administration of the ^{99m}Tc tin colloid, SNs were identified by the SPECT/CT system. This system was composed of a commercially available gantry-free SPECT with dual-head detectors (Skylight; ADAC Laboratories, Milpitas, Calif) and an 8 multidetector-row CT scanner (Light-Speed Ultra Instrument; General Electric, Milwaukee, Wis). The two instruments were juxtaposed so that the CT table bearing the patient could be moved directly into the SPECT scanner before CT scanning. As a result, each patient was identically positioned for SPECT and CT imaging.

SPECT data acquisition was performed with a vertex general-purpose parallel-hole (VXGP) collimator. A 360 SPECT scan was acquired and was followed by CT scanning. Reconstructive CT images were processed into Digital Imaging and Communications in Medicine (DICOM) data and then transferred to Pegasys (ADAC Laboratories, Milpitas, Calif), which is a workstation for SPECT processing. One lumen of a 3-way stopcock (inner diameter 4 mm, length 10 mm) containing an aqueous solution of ^{99m}Tc tin colloid and a contrast medium was used as an external fiducial marker. So that a precise record of both images could be obtained, external fiducial markers were fixed to the common platform for SPECT and CT imaging. The two scans were performed sequentially. Fusion of the SPECT images with the CT images was manually performed by aligning the external fiducial markers of the two images on the workstation, enabling localization of SN on CT images (Figure 1). An SN was visually identified on the F1 SPECT/CT images by two experienced radiologists before surgery (S.S. and K.K).

Gamma Probe Method

The radioactivity of the dissected lymph nodes was determined by a handheld gamma probe (Navigator; Auto Suture Japan, Tokyo, Japan), as reported previously.[4,5] An SN was defined as any node for which the radioactivity count was 10 times that of the background level.

Pathologic Examination

SNs were examined by intraoperative frozen section analysis using 2- to 3-mm thick sections. The dissected lymph nodes were examined histologically by use of formalin-fixed and paraffin-embedded sections with hematoxylin and eosin staining.

Statistical Analysis

Because the use of a gamma probe to measure radioactivity of dissected lymph nodes is now a standard method for SN identification, the sensitivity of SPECT/CT was examined on the basis of data gathered with the gamma probe, which was calculated as true positive/true positive + false negative. All data were analyzed for statistical significance by the χ^2 test. All values in the text and tables are given as mean ± standard deviation.

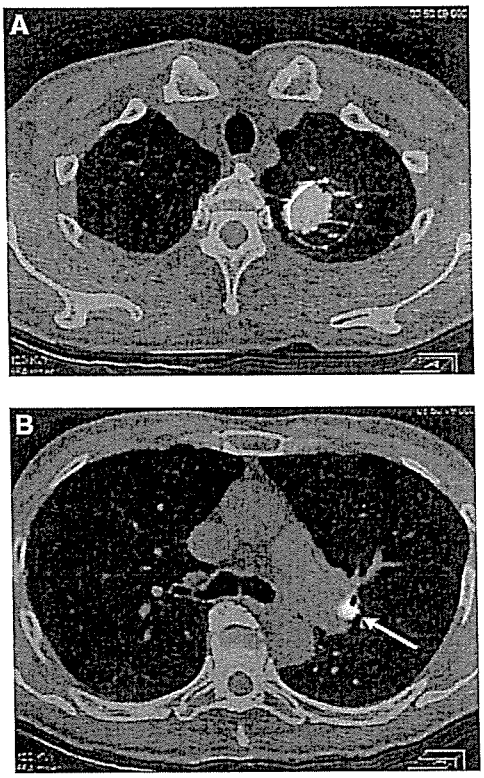

Figure 1. Fused SPECT/CT images in lung cancer of the left upper lobe. A, Primary tumor. B, Radiolabeled lymph node (segmental nodal station) can be detected *(arrow)*.

TABLE 1. Patient characteristics of SN identification by gamma probe

	Sentinel nodes by gamma probe	
	Identified	Not identified
Age (y)		
Mean ± SD	68 ± 7	74 ± 8*
Range	53-81	65-82
Sex (No.)		
Male	25	10
Female	24	4
Mean tumor size (mm)	19 ± 7	24 ± 8†
Tumor location (No.)		
Right upper lobe	13	3
Right middle lobe	2	1
Right lower lobe	8	3
Left upper lobe	17	5
Left lower lobe	9	2
Histologic type (No.)		
Adenocarcinoma	44	8
Squamous cell carcinoma	3	6
Adenosquamous carcinoma	1	0
Small cell carcinoma	1	0
Operative procedure (No.)		
Lobectomy	7	4
Segmentectomy	42	10
p-TNM (No.)		
T1 N0 M0	43	13
T2 N0 M0	1	1
T1 N1 M0	2	0
T1 N2 M0	3	0
Total	49	14

SN, Sentinel node. *P = .01; †P = .024.

Results

From April 2005 to September 2006, 79 patients with clinical stage Ia peripheral NSCLC underwent surgery at the Department of Thoracic Surgery of Kumamoto University Hospital. Of these, 16 patients could not be enrolled in this study because of the following reasons: (1) Preoperative histologic diagnosis was not obtained in 5 patients; (2) SPECT/CT could not be used because of the other examinations in 10 patients; and (3) one patient refused to participate in the study. As a result, 63 consecutive patients were enrolled in this study. The gamma probe identified SNs in 49 (78%) of the 63 patients, whose pathologic N stages were N0 in 44, N1 in 2, and N2 in 3 (Table 1). SPECT/CT could identify SNs in 39 (62%) patients, whose pathologic N stages were N0 in 34, N1 in 2, and N2 in 3 (Table 2). The SN identification rate by SPECT/CT imaging was lower than that achieved by the gamma probe with marginal significance (P = .052). The mean number of SNs identified by the gamma probe in the 48 patients was 1.6 ± 0.8 (range: 1-4); the value obtained by SPECT/CT in the 38 patients was 1.5 ± 0.6 (range: 1-3). However, there was no significant difference between the two methods in this respect.

Between the 49 patients with identifiable SNs and the 14 without by gamma probe, the mean age was younger and the mean tumor size was smaller in the former than in the latter, with significance (P = .01 and .024, respectively). However, there were no significant differences of other variables between patients with identifiable SNs and those without when both the gamma probe and SPECT/CT were used. Tumors in 2 patients were pathologically classified as T2: one tumor was involved over the pleura and the other one was larger than 3 cm in the permanent section. Although 2 patients needed tube drainage because of pneumothorax after the injection of the isotope, there were no other complications.

Table 3 shows the correlation between SPECT/CT imaging and the gamma probe method for SN identification at each nodal station of the hilum and mediastinum in the 49 patients whose SNs were identified by gamma probe. In the lymph node stations at the hilum, the gamma probe and SPECT/CT corresponded with each other in 46 (94%) patients at nodal station No. 10, 46 (94%) at No. 11, 42 (86%)

at No. 12, and 39 (80%) at No. 13. In the mediastinum of the right lung, the gamma probe and SPECT/CT corresponded with each other in 21 (91%) patients at nodal station No. 3, in 22 (96%) at No. 4, and in 22 (91%) at No. 7. In the mediastinum of the left lung, the gamma probe and SPECT/CT corresponded with each other in 26 (100%) patients at nodal station No. 4, in 22 (85%) at No. 5, and in 22 (85%) at No. 7. SNs were not identified at the other mediastinal nodal stations, that is, Nos. 1, 2, 8, and 9, using both methods.

The sensitivity of SPECT/CT based on Table 3 was 0.82 at nodal station No. 13, 0.74 at No. 12, 0.63 at No. 11, 0.40 at No. 10, and 0.31 at the mediastinal nodal stations (Figure 2). The sensitivity of SPECT/CT decreased numerically from nodal station No. 13 to No. 10 and was the lowest in the mediastinal lymph nodes. The sensitivity of SPECT/CT in the mediastinal lymph nodes was significantly lower than those at nodal station No. 13 and No. 12 ($P < .001$ and $P = .012$, respectively). The specificity of SPECT/CT based on Table 3 was 0.76 at No. 13, 0.93 at N0. 12, 1.0 at N0. 11, 1.0 at No. 10, and 0.99 at the mediastinum.

TABLE 2. Patient characteristics of SN identification by SPECT/CT

	SNs by SPECT/CT	
	Identified	Not identified
Age (y)		
Mean ± SD	68 ± 6	69 ± 7
Range	54-81	53-82
Sex (No.)		
Male	20	15
Female	19	9
Mean tumor size (mm)	19 ± 7	20 ± 7
Tumor location (No.)		
Right upper lobe	11	5
Right middle lobe	0	3
Right lower lobe	7	4
Left upper lobe	15	7
Left lower lobe	6	5
Histologic type (No.)		
Adenocarcinoma	34	18
Squamous cell carcinoma	4	5
Adenosquamous carcinoma	0	1
Small cell carcinoma	1	0
Operative procedure (No.)		
Lobectomy	5	6
Segmentectomy	34	18
pTNM (No.)		
T1 N0 M0	33	23
T2 N0 M0	1	1
T1 N1 M0	2	0
T1 N2 M0	3	0
Total	39	24

SN, Sentinel node; *SPECT/CT*, single photon emission computed tomography.

TABLE 3. Correlation between SPECT/CT and gamma probe for SN identification

	Patient number with SN identified by				
	Gamma probe (+)		Gamma probe (−)		
Station	SPECT (+) True positive	SPECT (−) False negative	SPECT (+) False positive	SPECT (−) True negative	Total
Hilum					
10	2	3	0	44	49
11	5	3	0	41	49
12	14	5	2	28	49
13	23	5	5	16	49
Mediastinum					
Right					
3	1	2	0	20	23
4	1	1	0	21	23
7	0	1	0	22	23
Left					
4	1	0	0	25	26
5	2	3	1	20	26
7	0	4	0	22	26

SN, Sentinel node; *SPECT/CT*, single photon emission computed tomography. +, Sentinel node is identified; −, sentinel node is not identified.

Pathologic examination showed lymph node metastases in 5 patients, that is, N1 in 2 patients and N2 in 3 (Table 4). Frozen section of the SNs identified by both SPECT/CT and the gamma probe could show metastases in all 5 patients.

Discussion

The present study showed that SPECT/CT was inferior to the gamma probe method for SN identification in the mediastinal lymph nodes. This discrepancy could be caused by the following: (1) the ability to measure radioactivity with SPECT/CT images is inferior to that of direct measurement

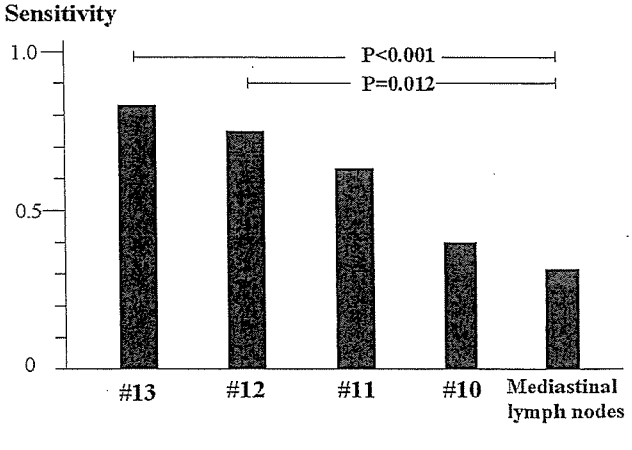

Figure 2. Sensitivity of SPECT/CT at each lymph node station.

TABLE 4. SNs identified by SPECT/CT and gamma probe in patients with N1 or N2 disease

No.	Age/sex	Tumor location	Histology	Metastatic node	SN		pTNM
					SPECT/CT	Gamma probe	
1	60/M	RLL	Ad	No. 13	No. 13	No. 13	T1 N1 M0
2	72/M	RLL	Ad	No. 11	No. 11	No. 11	T1 N1 M0
3	80/M	LUL	Ad	No. 5	No. 5	No. 5	T1 N2 M0
4	59/M	LUL	Ad	Nos. 5, 12, 13	Nos. 12, 13	Nos. 5, 12	T1 N2 M0
5	54/F	LLL	Ad	Nos. 7, 11, 12	Nos. 12, 13	No. 12	T1 N2 M0

SPECT/CT, Single photon emission computed tomography/computed tomography; *RLL*, right lower lobe; *LUL*, left upper lobe; *LLL*, left lower lobe; *Ad*, adenocarcinoma.

by a gamma probe and (2) the radioactivity of mediastinal SNs is usually lower than that of hilar SNs, because the former is further away from the primary tumor. Therefore, we conclude that SPECT/CT cannot easily identify SNs in the mediastinum. However, SPECT/CT could identify SNs at nodal station No. 12 and No. 13 with a sensitivity of 0.82 and 0.74, respectively. This may be because SNs at nodal station No. 12 and No. 13 are close to the primary tumor, which makes their radioactivity high enough for detection by SPECT/CT. In fact, in 5 patients with N1 or N2 disease, SPECT/CT imaged metastatic SNs in the hilum before the operation.

We[4] previously evaluated SN identification by using a gamma probe in 104 patients with clinical stage I NSCLC and concluded that although the gamma probe could identify SNs in the mediastinum before lymph node dissection (in vivo SN identification), it could not in the hilum owing to high radioactivity from primary tumors. Because the present study showed the usefulness of SPECT/CT for the in vivo SN identification in the hilum, we believe that the combination of SPECT/CT and the gamma probe could be useful for in vivo SN identification in both the hilum and the mediastinum.

Recently, it has been reported that segmentectomy could be an alternative to lobectomy for pathologic T1 N0 M0 NSCLC.[16,18,19] So that the final indication of segmentectomy can be determined, intraoperative frozen sections must be examined for all of the hilar and lobe-specific mediastinal lymph nodes to confirm the intraoperative N stage to be N0.[18,19] We consider that the application of SPECT/CT could be used for determining the final indication of segmentectomy as follows: (1) SNs identified in the hilum by SPECT/CT and those identified in the mediastinum by gamma probe are submitted for frozen sections; (2) when frozen sections of SNs show metastases, segmentectomy is converted to lobectomy. Even after segmentectomy, in vivo SN identification by gamma probe is usually difficult for the hilum owing to high radioactivity in the remaining segments. Therefore, if SPECT/CT is not used, all lymph nodes in the hilum have to be dissected during segmentectomy for SN identification by gamma probe, which is hard as well as time-consuming. On the other hand, for lobectomy, SN identification by SPECT/CT would not be necessary because lymph nodes at the hilum are routinely removed during lobectomy and can be examined for SN identification by gamma probe.

The sensitivities of SN identification at nodal station No. 10 and No. 11 by SPECT/CT were still low. Because station No. 10 is close to the mediastinum, the gamma probe can identify SNs at this station after resection of the primary tumor, as there will no longer be any interference of radioactivity from the primary tumor. Nodal station No. 11 is usually easy to excise even during segmentectomy, enabling SN identification by gamma probe.

Several tracers have been used for SN identification, such as ^{99m}Tc tin colloid, ^{99m}Tc sulfur colloid, and ^{99m}Tc phytate. Of these, ^{99m}Tc tin colloid has the largest particles, that is, about 1000 nm in diameter. The reason that we have used ^{99m}Tc tin colloid is as follows. Because the particles of tin colloid are large, they take longer to reach SNs than the other tracers with small particles. In lung cancer surgery, unlike operations for cancer in other organs, radioisotope injected frequently leaks into the tracheobronchus, which makes in vivo SN identification unreliable immediately after the injection. Because ^{99m}Tc tin colloid has to be injected a few hours before the operation to reach SNs, the material that leaked into the tracheobronchus is already washed out at surgery, resulting in more reliable in vivo SN identification than the other tracers with small particles.[4] We[4] previously confirmed that the radioactivity of ^{99m}Tc tin colloid in SNs was stable from 9 to 24 hours after the injection. On the other hand, ^{99m}Tc sulfur colloid can reach SNs rapidly because of their small particles, approximately 40 nm in diameter, but could pass through the true SNs and flow further up the chain of nodes, resulting in false negative results. Therefore, ^{99m}Tc sulfur colloid has to be injected immediately before surgery, which would make the in vivo SN identification difficult because of material leaking into the tracheobronchus. In fact, the previous reports using ^{99m}Tc sulfur colloid identified SNs in the dissected lymph nodes but not with in vivo identification.[6,7]

GTS

In conclusion, SPECT/CT can be used to identify SNs in the hilum before surgery, especially at nodal station No. 12 and No. 13, but not in the mediastinum. Because the gamma probe method can identify SN before lymph node dissection in the mediastinum but not in the hilum, a combination of SPECT/CT and the gamma probe could be used to identify SNs before lymph node dissection in both the hilum and the mediastinum. This will enable SN navigation surgery in patients with clinical stage Ia NSCLC, especially for segmentectomy.

References

1. Tafra L, Lannin DR, Swanson MS, Eyk JJV, Verbanac KM, Chua AN, et al. Multicenter trial of sentinel node biopsy for breast cancer using both technetium sulfur colloid and isosulfan blue dye. *Ann Surg.* 2001; 233:51-9.
2. Morton DL, Thompson JF, Essner R, Elashoff R, Stern SL, Nieweg OE, et al. Validation of the accuracy of intraoperative lymphatic mapping and sentinel lymphadenectomy for early–stage melanoma. *Ann Surg.* 1999;230:453-65.
3. Kitagawa Y, Fujii H, Mukai M, Kubota T, Ando N, Watanage M, et al. The role of the sentinel lymph node in gastrointestinal cancer. *Surg Clin North Am.* 2000;80:1799-809.
4. Nomori H, Watanabe K, Ohtsuka T, Naruke T, Suemasu K. In vivo identification of sentinel nodes for clinical stage I non-small cell lung cancer for abbreviation of mediastinal lymph node dissection. *Lung Cancer.* 2004;46:49-55.
5. Nomori H, Horio H, Naruke T, Orikasa H, Yamazaki K, Suemasu K. Use of technetium-99m tin colloid for sentinel lymph node identification in non–small cell lung cancer. *J Thorac Cardiovasc Surg.* 2002; 124:486-92.
6. Liptay MJ, Masters GA, Winchester DJ, Edelman BL, Carrido BJ, Hirshctritt TR, et al. Intraoperative radioisotope sentinel lymph node mapping in non-small cell lung cancer. *Ann Thorac Surg.* 2000;70: 384-90.
7. Liptay MJ, Grondin SC, Fry WA, Pozdol C, Carson D, Knop C, et al. Intraoperative sentinel lymph node mapping in non-small cell lung cancer improves detection of micrometastases. *J Clin Oncol.* 2002;20: 1984-8.
8. Schmidt FE, Woltering EA, Webb WR, Garcia OM, Cohen JE, Rozans MH. Sentinel nodal assessment in patients with carcinoma of the lung. *Ann Thorac Surg.* 2002;74:870-4.
9. Melfi FM, Chella A, Menconi GF, Givigliano F, Boni G, Mariani G, et al. Intraoperative radioguided sentinel lymph node biopsy in non-small cell lung cancer. *Eur J Cardiothorac Surg.* 2003;23:214-20.
10. Sugi K, Kaneda Y, Sudoh M, Sakano H, Hamano K. Effect of radioisotope sentinel node mapping in patients with cT1 N0 M0 lung cancer. *J Thorac Cardiovasc Surg.* 2003;126:568-73.
11. Carlson GW, Murray DR, Greenlee R, Alazraki N, Fry-Spray C, Poole R, et al. Management of malignant melanoma of the head and neck using dynamic lymphoscintigraphy and gamma-probe-guided sentinel lymph node biopsy. *Arch Otolaryngol Head Neck Surg.* 2000;126: 433-7.
12. de Wilt HW, Thompson JF, Uren RF, Ka VS, Scolyer RA, McCarthy WH, et al. Correlation between preoperative lymphoscintigraphy and metastatic nodal disease sites in 362 patients with cutaneous melanoma of the head and neck. *Ann Surg.* 2004;239:544-52.
13. Albertini JJ, Cruse CW, Rapaport D, Wells K, Ross M, DeConti R, et al. Intraoperative radio-lymphoscintigraphy improves sentinel lymph node identification for patients with melanoma. *Ann Surg.* 1996;223: 217-24.
14. Ishihara T, Kaguchi A, Matsushita S, Shiraishi S, Tomiguchi S, Yamashita Y, et al. Management of sentinel lymph nodes in malignant skin tumors using dynamic lymphoscintigraphy and the single-photon-emission computed tomography/computed tomography combined system. *Int J Clin Oncol.* 2006;11:214-20.
15. Nomori H, Horio H, Naruke T, Suemasu K. What is the advantage of a thoracoscopic lobectomy over a limited thoracotomy procedure for lung cancer surgery? *Ann Thorac Surg.* 2001;72:879-84.
16. Nomori H, Ikeda K, Mori T, Kobayashi H, Iwatani K, Kawanaka K, et al. Sentinel node navigation segmentectomy for c-T1 N0 M0 non–small cell lung cancer. *J Thorac Cardiovasc Surg.* ~~In press.~~ 2007 133 : 780-5 AQ: 2
17. Naruke T, Suemasu K, Ishikawa S. Lymph node mapping and curability at various levels of metastasis in resected lung cancer. *J Thorac Cardiovasc Surg.* 1978;76:832-9.
18. Okada M, Yoshikawa K, Hatta T, Tsubota N. Is segmentectomy with lymph node assessment an alternative to lobectomy for non-small cell lung cancer of 2 cm or smaller? *Ann Thorac Surg.* 2001;71:956-61.
19. Yoshikawa K, Tsubota N, Kodama K, Ayabe H, Taki T, Mori T, et al. Prospective study of extended segmentectomy for small lung tumors: the final report. *Ann Thorac Surg.* 2002;73:1055-9.